

1 **Supplementary Information**

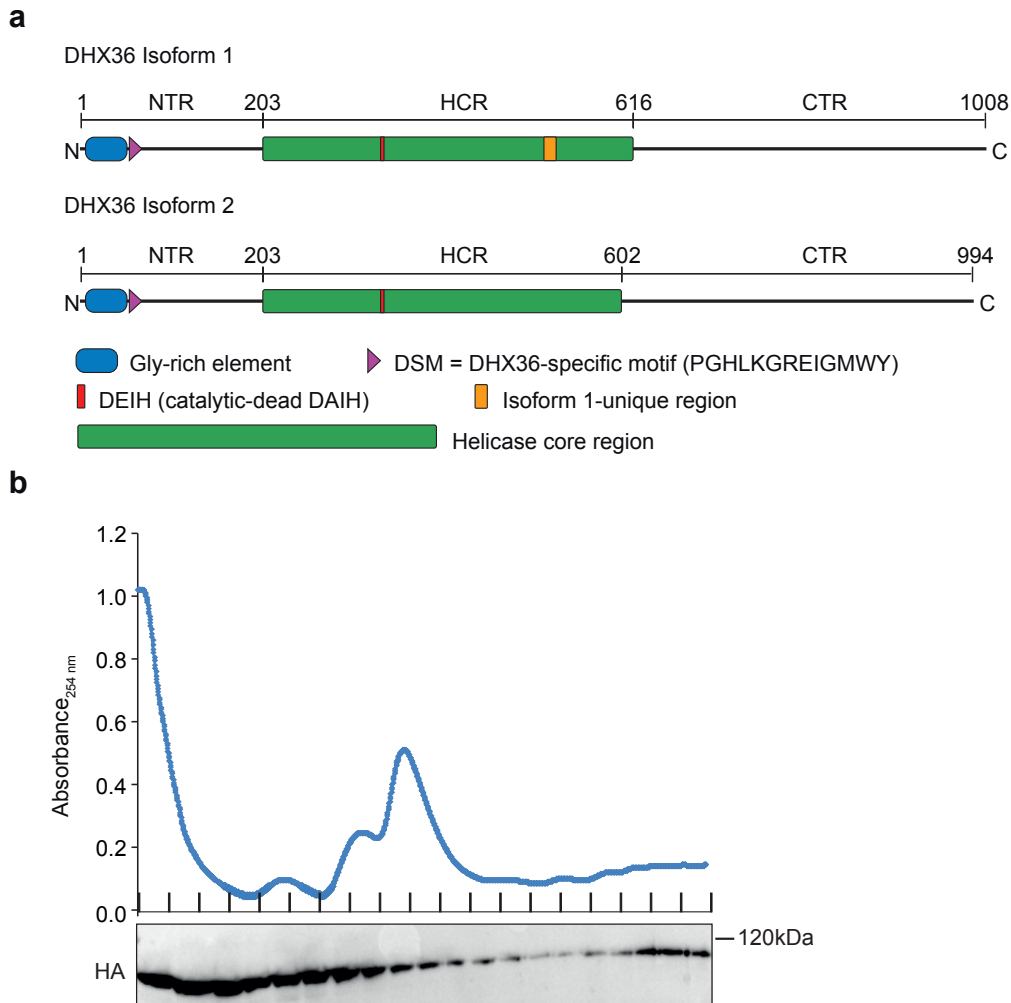
2 **DHX36 prevents the accumulation of translationally inactive mRNAs with G4-**  
3 **structures in untranslated regions**

4 Sauer, Juranek, Marks, De Magis et al.

5 Supplementary Figures (1-9) and Supplementary Table 1

6

7 **Supplementary Figures**



8

9 **Supplementary Figure 1. Schematic of DHX36 isoforms and DHX36 overexpression polysome**

10 **gradient. a**, Schematic representation of DHX36 isoforms 1 and 2. The RNA binding Gly-rich element

11 (blue) and DHX36-specific motif (DSM) (purple) are indicated. 14 additional aa in the helicase core

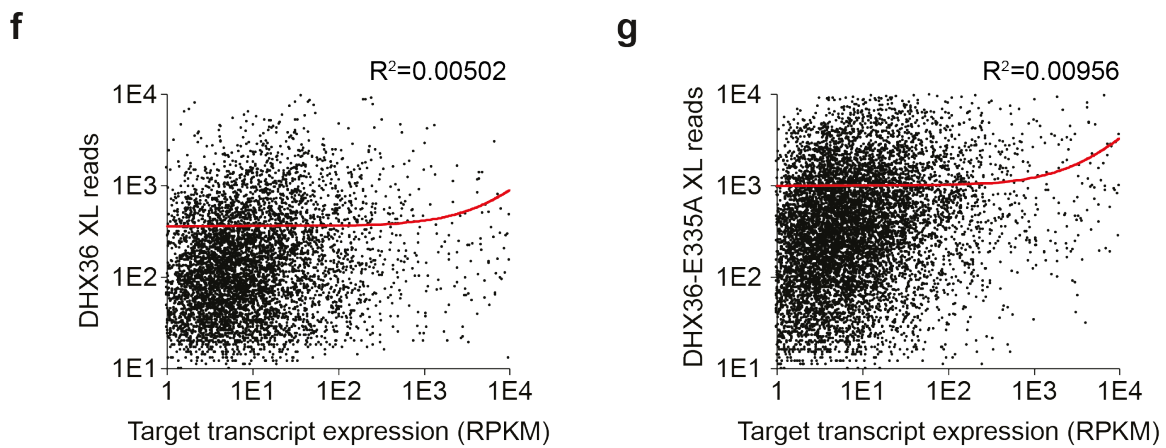
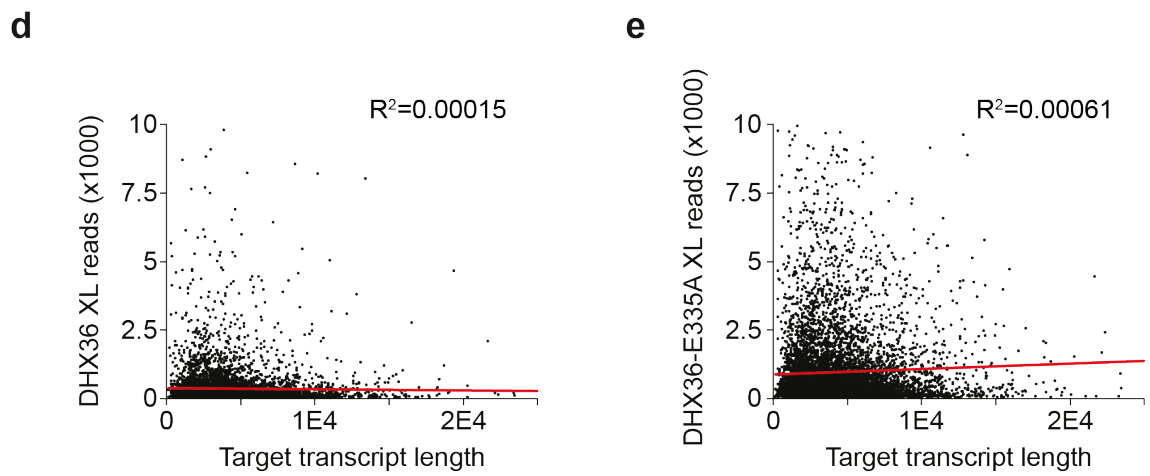
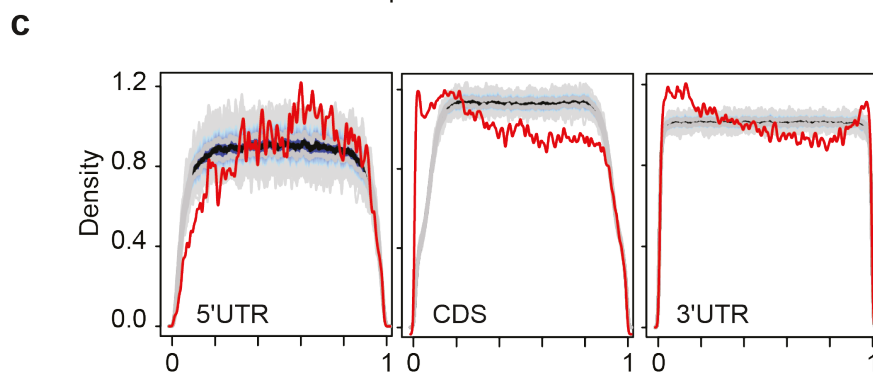
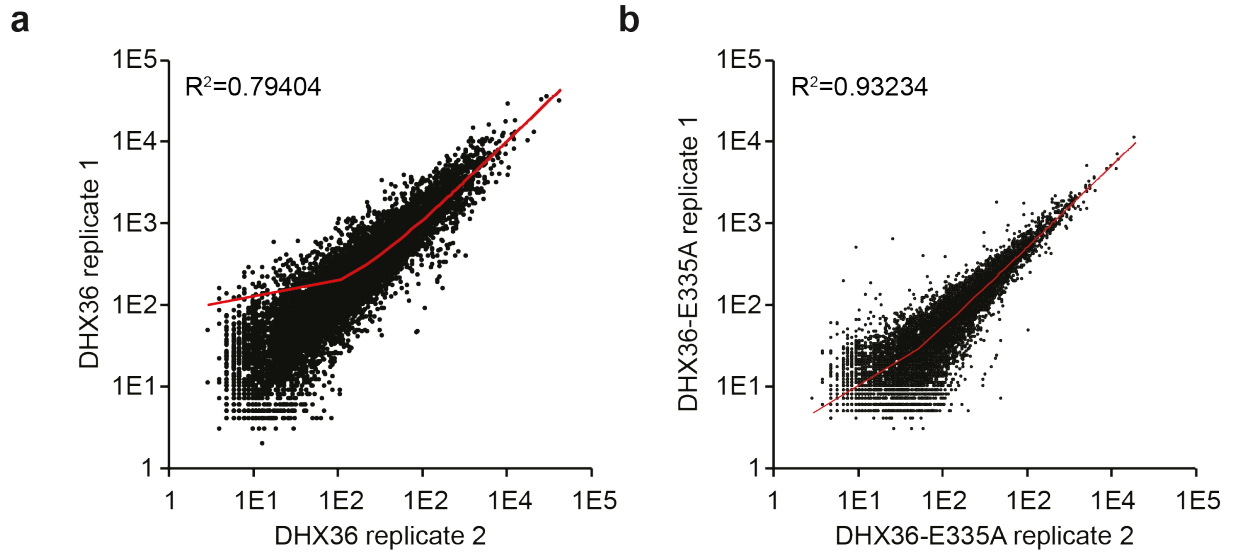
12 region (green) of isoform 1 are marked (orange). The conserved Walker-B box is indicated in red

13 (wildtype sequence: DEIH, catalytically inactive mutant sequence: DAIH). **b**, UV absorbances at 254 nm

14 DHX36 overexpression HEK293 cell extracts separated by sucrose gradient centrifugation are shown.

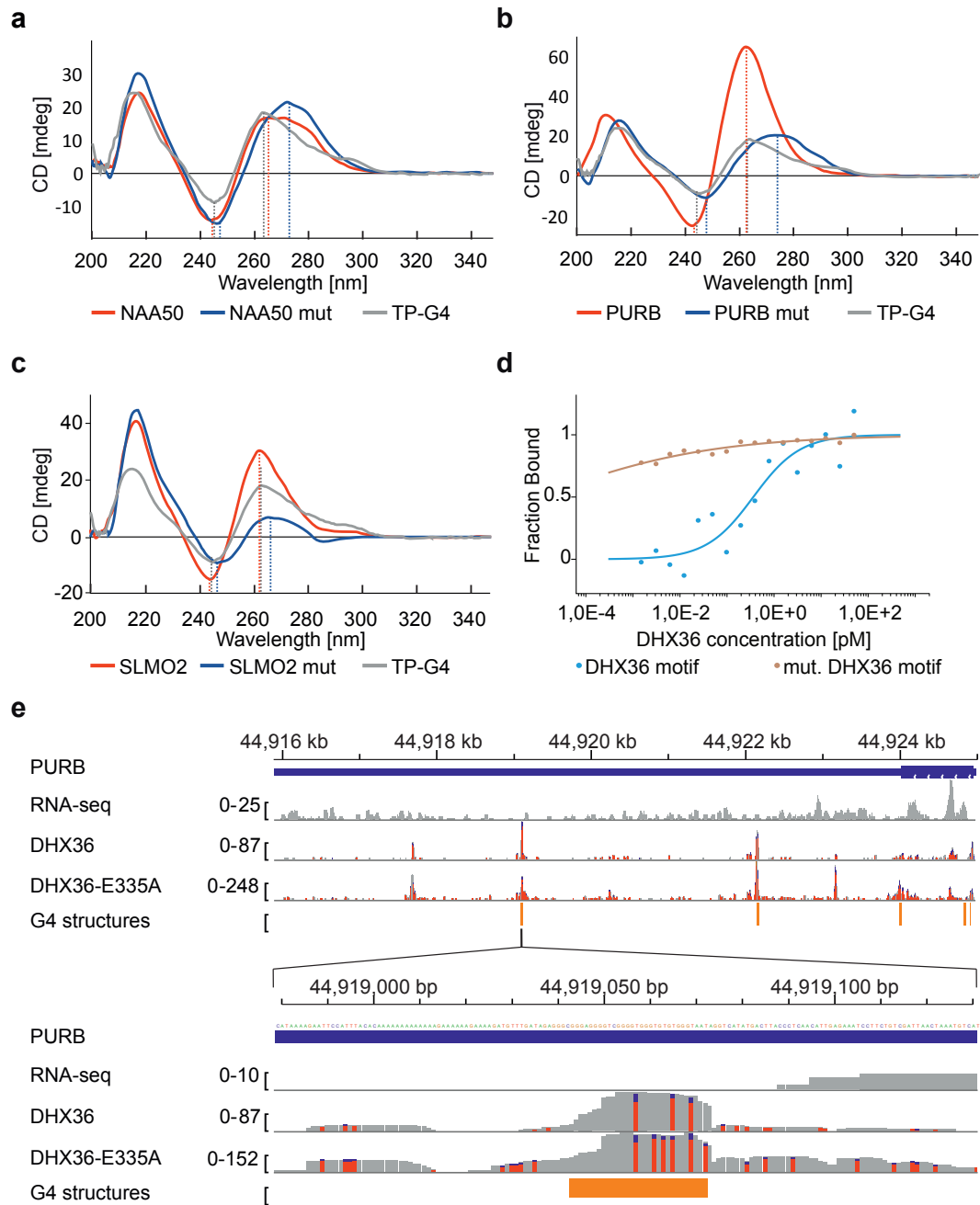
15 Western blot probed for FH-DHX36 is shown below. Source data are provided as a Source Data file.

16



18 **Supplementary Figure 2. Replicates of FH-DHX36 and FH-DHX36-E335A PAR-CLIPs and binding**  
19 **determinants. a - b**, The correlation of crosslinked reads from the biological replicates of FH-DHX36  
20 **(a)** or FH-DHX36-E335A **(b)** PAR-CLIP experiments is shown. **c**, DHX36 binds preferentially close to  
21 the start and the stop codon based on a metagene analysis of the distribution of DHX36 binding clusters  
22 on mRNAs subdivided into 5' UTR, CDS, and 3' UTR (red lines). The distribution of 1,000 mismatched  
23 randomized controls is shown in gray lines. **d – g**, DHX36 binding on target mRNA is not determined by  
24 target transcript length or expression. **d - e**, Correlation between crosslinked reads from FH-DHX36  
25 PAR-CLIP **(d)** or FH-DHX36-E335A PAR-CLIP **(e)** and target transcript length. Correlation coefficients  
26 ( $R^2$ ) are indicated. **f - g**, DHX36 binding on target mRNA is also not determined by target transcript  
27 expression. Correlation of DHX36 binding with target transcript expression from FH-DHX36 PAR-CLIP  
28 **(f)** or FH-DHX36-E335A PAR-CLIP **(g)**.  
29





30

31 **Supplementary Figure 3. DHX36 binds at G-rich sites which can form a parallel G-quadruplex *in***

32 ***vitro*. a - c**, Circular dichroism measurements of oligonucleotides representing native DHX36 RRE of

33 the NAA50 (a), PURB (b), and SLMO2 (c) mRNAs after performing the G4-folding protocol. Positive

34 control TP-G4) is indicated in gray, wildtype RREs in red, and mutated RREs in blue. Lines represent

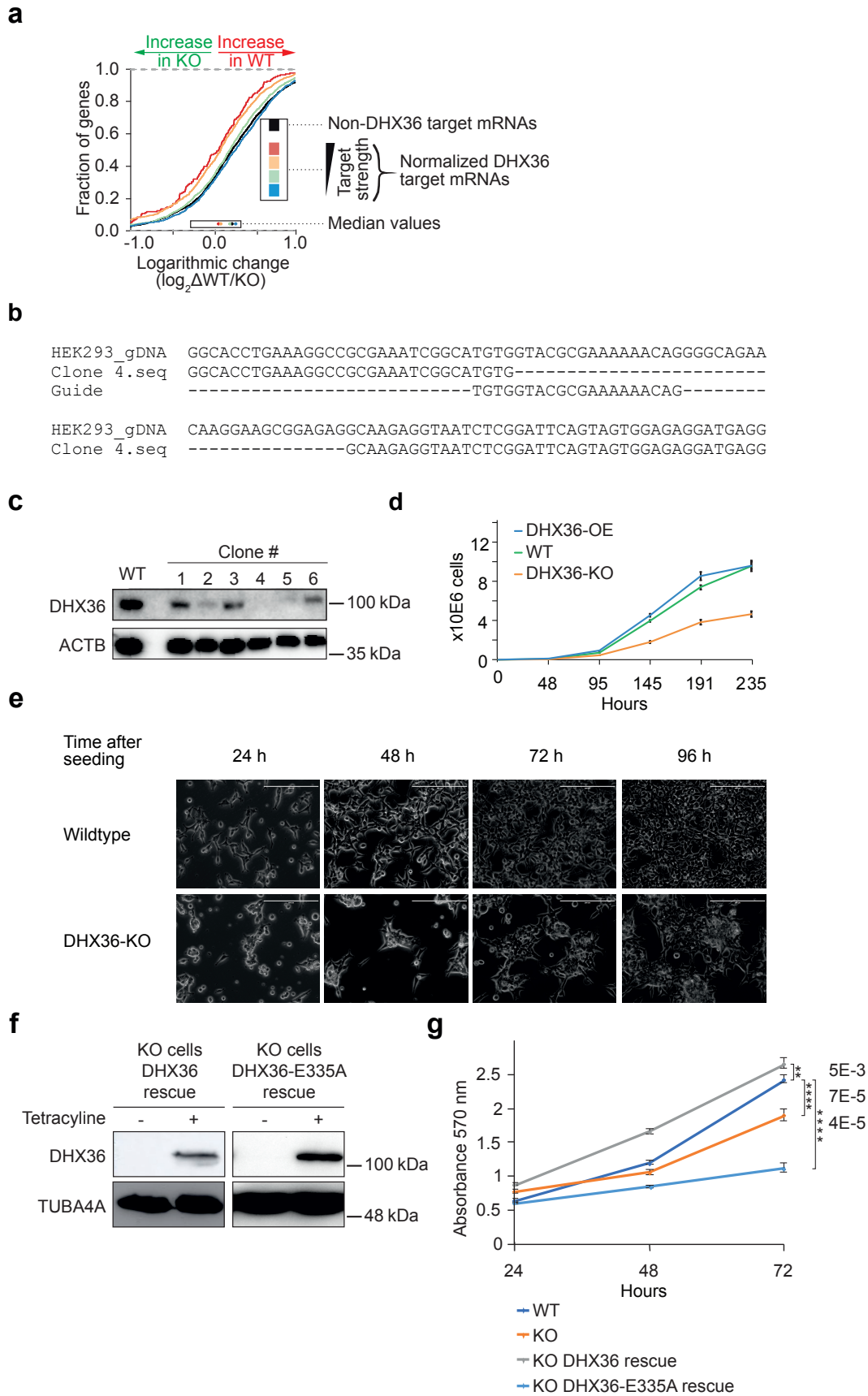
35 mean of ten subsequent measurements. Sequences of oligonucleotides are listed Suppl. Table S7. d,

36 Microscale thermophoresis analysis shows binding of DHX36 to the DHX36-binding motif (Cy5-

37 AAAAAGGAGGAGGAGGAGG) but not to the mutated motif (Cy5-AAAAAGCAGCAGGAGCAGCA). e,

38 Top panel: Screenshots of the FH-DHX36 and FH-DHX36-E335A PAR-CLIP binding sites for the

39 representative target gene PURB. The gene structure is shown, as well as coverage from a HEK293  
40 RNA-seq experiment. The bottom two tracks show the alignment of sequence reads with characteristic  
41 T-to-C mutations from a FH-DHX36 and FH-DHX36-E335A PAR-CLIP experiment. Bottom panel:  
42 Close-up of the indicated region in the 3' UTR of PURB. Source data are provided as a Source Data file.  
43

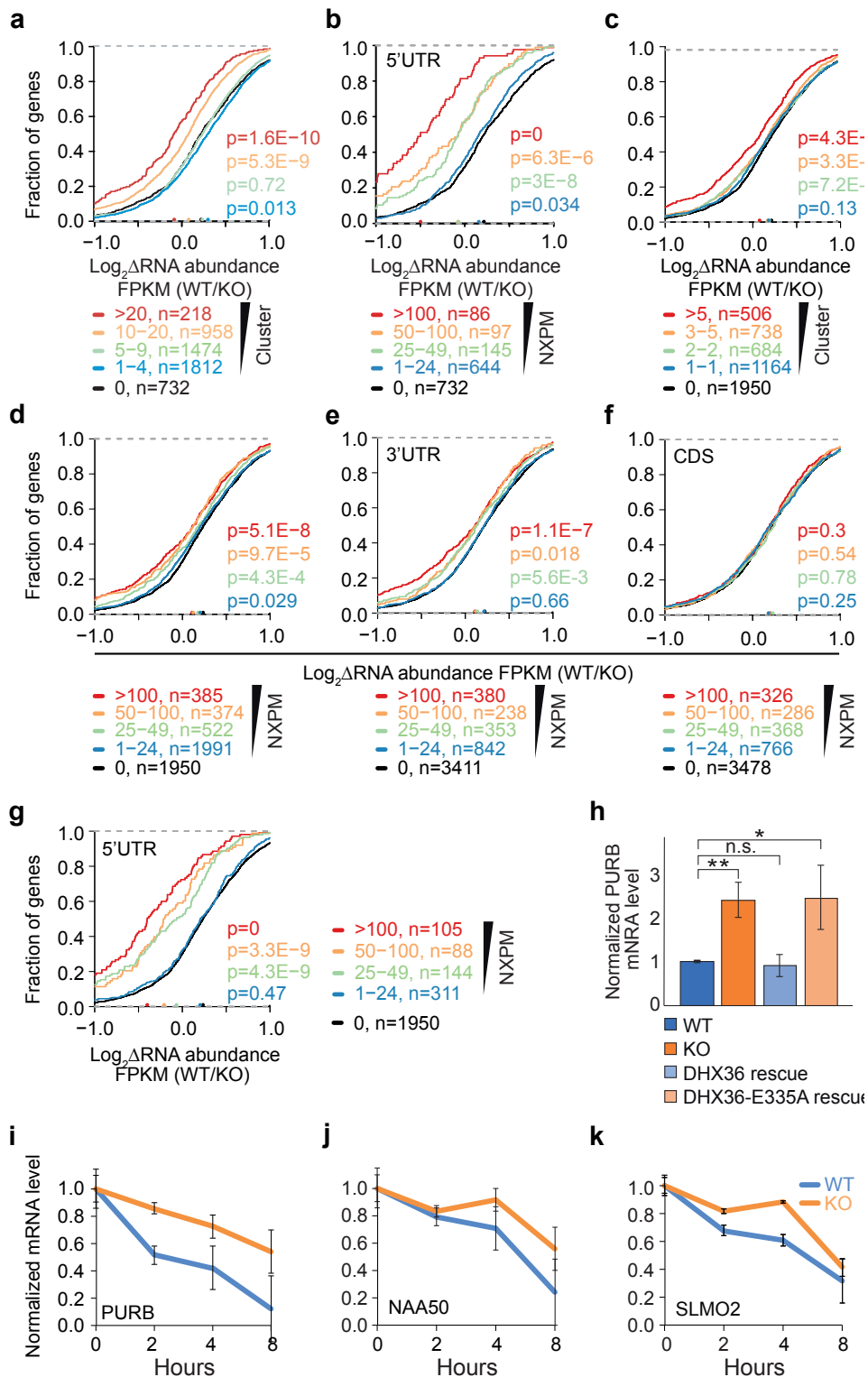


44

45 **Supplementary Figure 4. Characterization of the DHX36-KO cell line.** a, Schematic explanation of  
 46 cumulative distribution functions (CDFs). mRNAs are grouped in “DHX36 non-targets” (black line) and

47 according to the binding strength sorted by colors (red, yellow, green, and blue) represented by  
48 normalized crosslinked reads per million (NXPM) or the number of binding sites (clusters, in the  
49 Supplements). Conditions of binning, number (n) and significances are indicated. Fractions of genes  
50 are blotted against the logarithmic change of wildtype over DHX36-KO. Shifting of a colored line to the  
51 left compared to the non-targets (black) means higher amounts in wildtype compared to the DHX36-KO  
52 and shifting to the right means higher amounts in DHX36-KO compared to wildtype, respectively.  
53 Colored dots on the x-axis represent median values. **b**, Sequence of genomic DNA of DHX36 knockout  
54 clone indicates the disruption of the gene. Sequence of guide RNA (gRNA) is indicated. **c**, Western blot  
55 screening after Cas9-mediated gene editing shows that DHX36 was knocked out in clones 4 and 5.  
56 ACTB serves as loading control. **d**, DHX36-KO cells have a growth defect compared to wildtype. Error  
57 bars represent standard deviations of three independent experiments. **e**, Changes in morphology of  
58 DHX36-KO cells compared to parental wildtype HEK293 cells. KO cells are not able to equally spread  
59 over the culture plate surface. Images were taken at indicate timepoints after seeding. Bar represents  
60 200  $\mu\text{m}$ . **f**, Generation of DHX36-KO cells stably expressing FH-DHX36 or FH-DHX36-E335A,  
61 respectively, upon tetracycline induction. **g**, MTT-proliferation assay depicted by blotting absorbance at  
62 570 nm (maximum of the formazan product) over time (range of 72 h). HEK293 WT cells have higher  
63 proliferation rates compared to DHX36-KO cell. KO cells overexpressing DHX36-E335A have even  
64 lower proliferation rates as paternal DHX36-KO cells. Proliferation rates of KO cells overexpressing  
65 DHX36 exceed wildtype rates (n=3). Error bars represent standard deviations of four independent  
66 experiments. Source data are provided as a Source Data file.

67

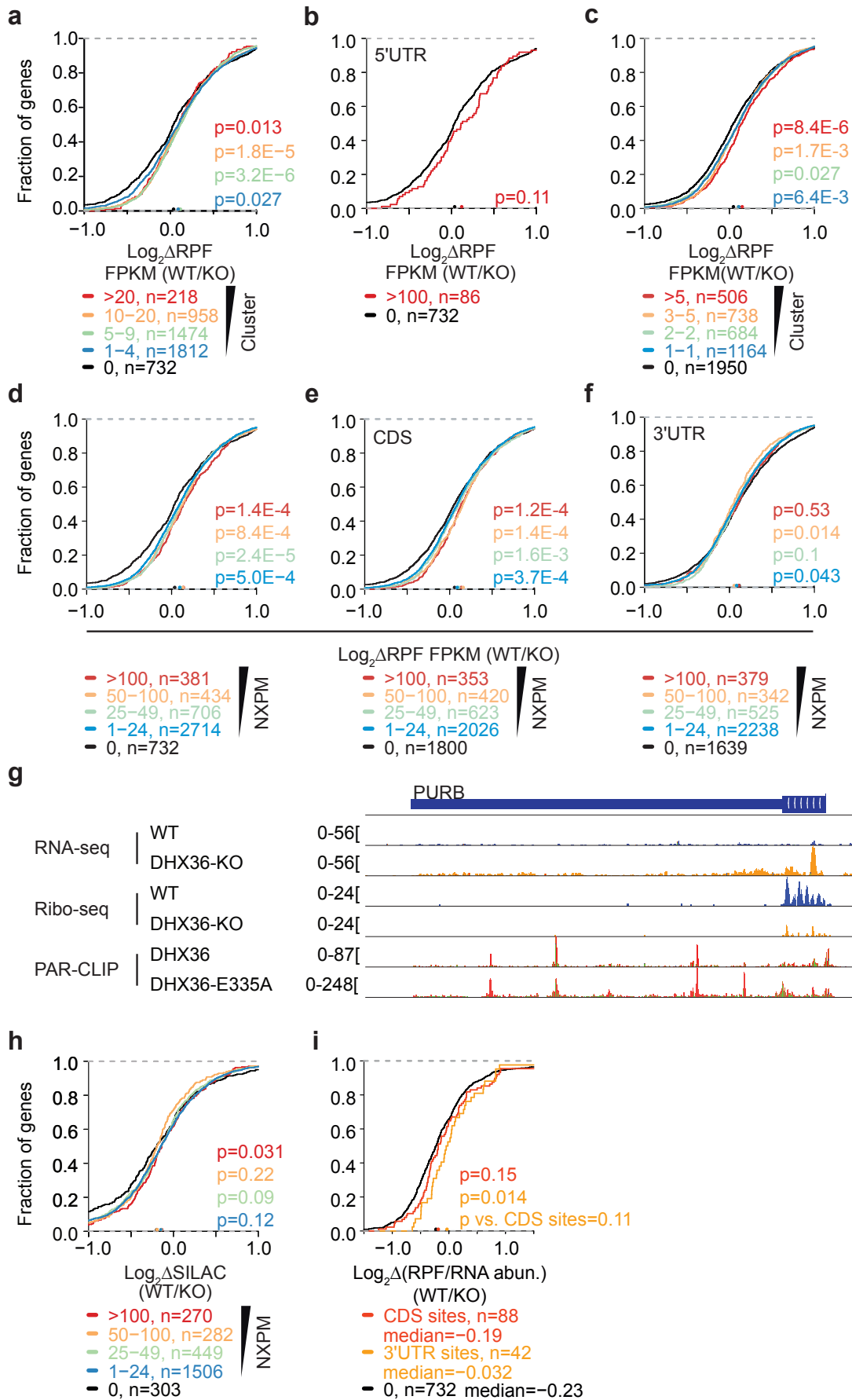


68

69 **Supplementary Figure 5. Detailed integration of PAR-CLIP with RNA-seq data. a**, Same as in **Fig.**  
 70 **4a**, except mRNAs were binned based on the number of binding clusters. **b**, Same as in **Fig. 4a**, except  
 71 mRNAs were binned based on the number of NXPM in the 5' UTR. **c**, Same as in **a**, except FH-DHX36  
 72 wildtype PAR-CLIP data were used. **d**, Same as in **Fig. 4a**, except FH-DHX36 wildtype PAR-CLIP data  
 73 were used. **e**, Same as in **Fig. 4c**, except FH-DHX36 wildtype PAR-CLIP data were used. **f**, Same as

74 in **Fig. 4b**, except FH-DHX36 wildtype PAR-CLIP data were used. **g**, Same as in **b**, except FH-DHX36  
75 wildtype PAR-CLIP data were used. **h**, Same as in **Fig. 4e**, except analyzing PURB mRNA levels. **l - k**,  
76 Same as in **Fig. 4g** except DHX36 binding target mRNAs PURB (**i**), NAA50 (**j**), and SLMO2 (**k**) were  
77 analyzed. Error bars represent standard deviations of three independent experiments. Source data are  
78 provided as a Source Data file.

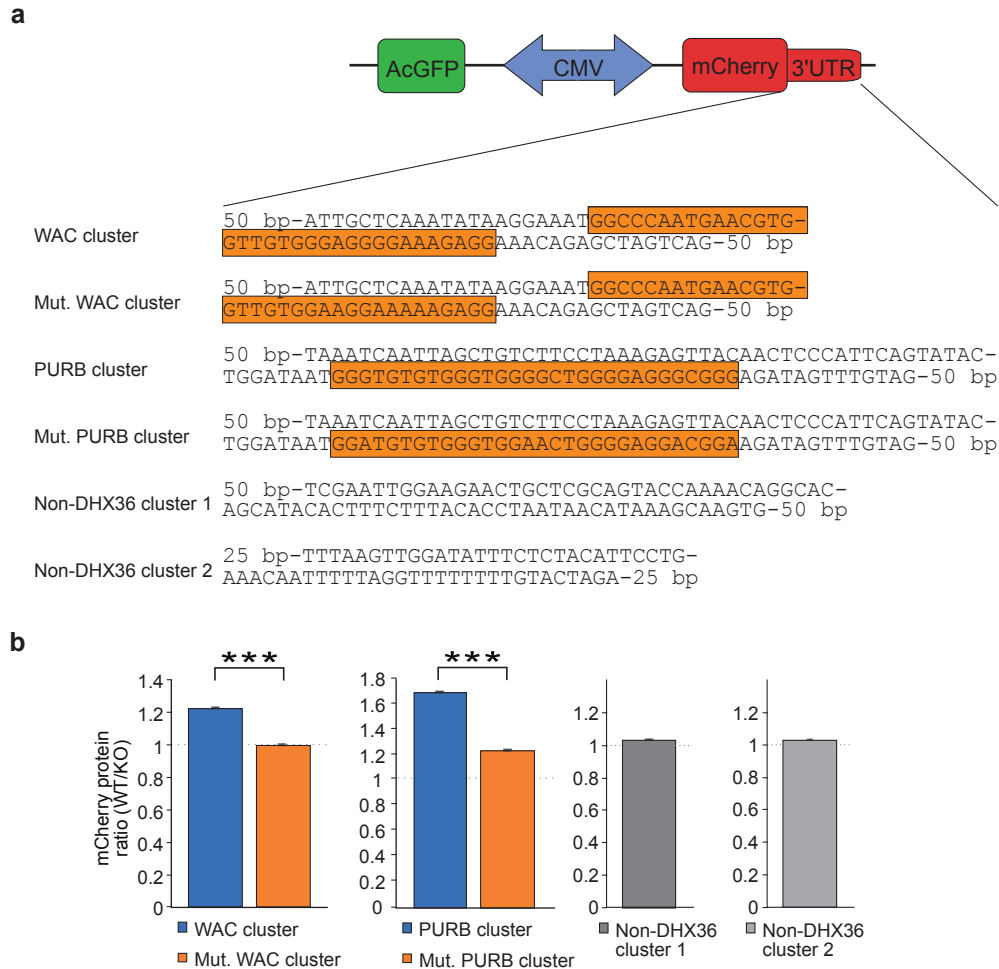
79



81 **Supplementary Figure 6. Detailed integration of PAR-CLIP data and RNA/Ribo-seq.** **a**, Same as in  
82 **Fig. 5a**, except mRNAs were binned based on the number of binding clusters. **b**, Same as in **Fig. 5a**,  
83 except mRNAs were binned based on the number NXPM in the 5' UTR. **c**, Same as in **a**, except FH-  
84 DHX36 wildtype PAR-CLIP data were used. **d**, Same as in **Fig. 5a**, except FH-DHX36 wildtype PAR-  
85 CLIP data were used. **e**, Same as in **Fig. 5b**, except FH-DHX36 wildtype PAR-CLIP data were used. **f**,  
86 Same as in **Fig. 5c**, except FH-DHX36 wildtype PAR-CLIP data were used. **g**, Same as **Fig. 5e** except  
87 the PURB mRNA binding site is depicted. **h**, Same as in **Fig. 5d**, except FH-DHX36 wildtype PAR-CLIP  
88 data were used. **i**, Cumulative distribution function comparing changes in DHX36 target mRNA  
89 abundance of DHX36 knockout cells (n=3) and parental HEK293 cells (n=3). DHX36-target mRNAs  
90 (determined by binding clusters) are separated by coding-sequence bound and 3' UTR bound.

91





92

93 **Supplementary Figure 7. Reporter assays for functional dissection of individual PAR-CLIP**

94 **binding sites. a**, Schematic representation of the reporter gene construct stable integrated in HEK293

95 wildtype and DHX36-KO cells. AcGFP and mCherry are co-expressed under the control of a bidirectional

96 CMV promoter. Native WAC and PURB binding clusters (highlighted in orange) in their natural sequence

97 context (+ 50 bp upstream and downstream) are indicated as well as mutated versions (G to A mutations

98 in bold) and non-binding clusters of DHX36 **b**, Ratios of mCherry protein levels in WT and DHX36-KO

99 cells expressed from the stably integrated reporter gene constructs determined by flow cytometry.

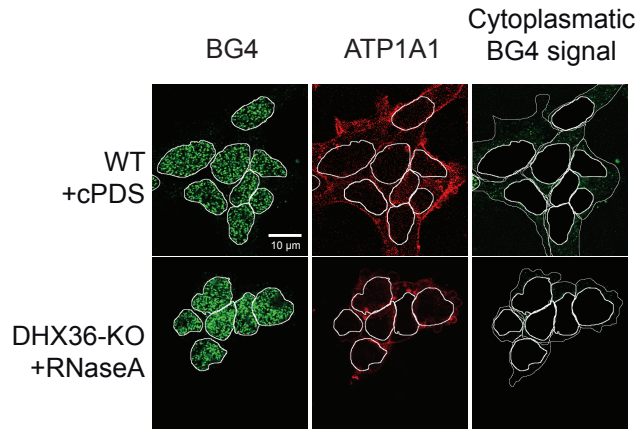
100 Median fluorescence intensities (MFI) of three times 100,000 double positive cells were analyzed. Error

101 bars represent standard deviations of three experiments. Significance was calculated using a Student's

102 T-Test (n=3) Significance levels: \* $P < 0.05$ , \*\* $P < 0.01$ , and \*\*\* $P < 0.001$ . Source data are provided as a

103 Source Data file.

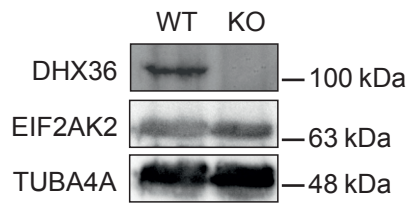
104



105

106 **Supplementary Figure 8. Detailed microscopic images for the quantification in Fig. 6.**

107



108

109 **Supplementary Figure 9. DHX36 KO does not result in overall elevated PKR levels.**

110 Western blot analysis of wildtype HEK293 cells (WT), DHX36-KO cells (KO) probed with antibodies

111 directed against DHX36, PKR (EIF2AK2); and TUBA4A as loading control. Source data are provided as

112 a Source Data file.

113

114 **Supplementary Table 1**

115

116 Oligonucleotides used in this study

Name	Sequence
Cloning of DHX36	
For DHX36	GGATCCGGATCCATGAGTTATGACTACCATCAG
Rev DHX36	CTCGAGCTCGAGTCAGCTGTAATATCCATCCTG
For DHX36-E335A	GTACTTGATGCAATCCATGAAAGAAATCGCAGTCAG
Rev DHX36-E335A	CATGGATTGCATCAAGTACGATATGACTAACACTGGAC
For DHX36-Del14	GATCTCTTGATGTCACAAGTAATGTTTAAATCAGTTAACAGACACAGGTGTT TAAAAGAACCCTCCTGGTGTTCGGAAAATAGTAATTGC
Rev DHX36-Del14	GGGGTTCTTTTAAACACCTGTGTCTGGTTAACTGATTTAAACATTACTTGTGA CATCAAGAGATCATGTAAGTGCTGATATTGTCCCAGCCTGG
Cloning of reporter constructs	
For GWC PURB	GGGGACAAGTTTGTACAAAAAAGCAGGCTTCATAGTAAGTGAATGAGATTATC AG
Rev GWC PURB	GGGGACCACTTTGTACAAGAAAGCTGGGTGCTGTATTTTCTTAAGGTAAATGT G
For GWC WAC	GGGGACAAGTTTGTACAAAAAAGCAGGCTTCAATGGACTTAAAAGTACTGCTG GATCGCTCAATGGACTTAAAAGTACTGCTG
Rev GWC WAC	GGGGACCACTTTGTACAAGAAAGCTGGGTGAACAATTTTGTGTTGTTTAAACA TG
For PURB mut RF	CAATTAGCTGTCTTCCATAAGAGTTACAACCTCCATTCACTAGTATACTGGATAAT GAGTGTGTGGGTGAAGCTG
Rev PURB mut RF	CTTAAGGTAAATGTGTTTTTTTTTTTTTCTTTTTTCTTTTCTACAACTATCT CTCGCTCTCCCAGCTTC
For WAC mut RF	GACAGGCATGTGTGCTCAAAGTACATTGATTGCTCAAATATAAGGAAATGGCC CAATGAACGTGGTTG
Rev WAC mut RF	GTTTTATTACAACAGATACAATTACATCTGACTAGCTCTGTTTCTCTTTCTTT CTCTCACAAAC
For non-target site 1	GGGGACAAGTTTGTACAAAAAAGCAGGCTTCAAATTTGTCATCAATTATGACT ACCC
Rev non-target site 1	GGGGACCACTTTGTACAAGAAAGCTGGGTGTTGGGATTAATTGCTTGATTAGC
For non-target site 2	GGGGACAAGTTTGTACAAAAAAGCAGGCTTCGTAATTATGGTGCACTTTTTCG
Rev non-target site 2	GGGGACCACTTTGTACAAGAAAGCTGGGTGTTTTGTGAAAACACTGCCTGC
CD oligonucleotides	
PAR-CLIP derived RRE	GGAGGAGGAGGAGG
mutated PAR-CLIP derived RRE 1	GAAGAAGGAGAAGAA
mutated PAR-CLIP derived RRE 2	GCAGCAGGAGCAGCA

TP-G4 (positive control)	GGGGGAGCTGGGGTAGATGGGAATGTGAGGG
WAC RRE	GGCCAATGAACGTGGTTGTGGGAGGGAAAGAGG
mutated WAC RRE	GGCCAATGAACGTGGTTGTGAGAGAAGAAAGAGG
PURB RRE	GGGTGTGTGGGTGGGGCTGGGGAGGGCGGG
mutated PURB RRE	GAGTGTGTGGGTGAAGCTGGGGAGAGCGAG
NAA50 RRE	GGGGACTGCACAAGGATGTGAATACTGGGAGGTGG
mutated NAA50 RRE	GGGACTGCACAAGGATGTGAATACTGAGAGGTGG
SLMO2 RRE	GGTGGGAAGAACAAGCATAATGGTAGGGGAGG
mutated SLMO2 RRE	GGTGAGAAGAACAAGCATAATGGTAGAGAGAGG
MST	
DHX36 motif 5' link Cy5	AAAAAGGAGGAGGAGGAGGA
DHX36 motif mut2 5' link Cy5	AAAAAGCAGCAGGAGCAGCA
qPCR primer	
For RNU6 RT	GCTTCGGCAGCACATATACTAAAAT
Rev RNU6 RT	CGCTTCACGAATTTGCGTGTCTAT
For NAA50 RT	TGGCACCTTACCGAAGGCTA
Rev NAA50 RT	TTGCCGACTCATTGCTGATCT
For PURB RT	GCCATCACCGTACCCTTCAAA
Rev PURB RT	CCCTCTGTCGTTCCCTGGATTT
For WAC RT	GCCGGAGATCCTTCACCAC
Rev WAC RT	TTTGGCCTTACTGTGACCTGT
For SLMO2 RT	CCCAAACCTATGAACCCAAG
Rev SLMO2 RT	TGTGCAACTTCCAGAGGG
For mCherry RT	CCCGCCGACATCCCCGACTA
Rev mCherry RT	GGGTCACGGTCACCACGCC

117

118